

Thermal environment and UV-B radiation indices in the Vojvodina region, Serbia

S. Malinovic-Milicevic^{1,*}, D. T. Mihailovic², B. Lalic², N. Dreskovic³

¹ACIMSI, University Center for Meteorology and Environmental Modelling, University of Novi Sad, Dositeja Obradovica Sq. 5, 21000 Novi Sad, Serbia

²Faculty of Agriculture, University of Novi Sad, Dositeja Obradovica Sq. 8, 21000 Novi Sad, Serbia

³Faculty of Sciences, Department of Geography, University of Sarajevo, Zmaj from Bosnia 33-35, 71000 Sarajevo, Bosnia and Herzegovina

ABSTRACT: We considered thermal environment and UV-B radiation indices in the Vojvodina region, Serbia. We derived an empirical formula for estimating the daily sum of the UV-B from global radiation and used this formula to reconstruct the UV-B radiation pattern for 1981–2008. We describe the actual climate conditions for the period 1992–2008. In addition, we applied a statistical downscaling technique on ECHAM5 outputs under the A2 scenario to assess the 2040 climate. The results indicate that a warmer and drier climate in the Vojvodina region can be expected because of the following evidence: an increase in the mean annual temperature (8.6 to 12.3%) and in the frequency of hot days (29.4 to 50%); a decrease in the mean annual precipitation (8.1 to 14.2%) and in the frequency of cold days (11.8 to 27.8%); a higher increase in the mean temperature for the colder period (24.9%) than for the hotter one (6.7%); and a reduction in precipitation during the growing season (15.7%). We have analyzed the thermal environment for the period 1992–2008 using the wind chill index and the heat index for the winter (December to February) and summer (June to August) periods. In all places, the heat index has a tendency for growth. We determined an increase in the daily UV-B dose in an amount of 3.7% per decade. Even though there is some evidence indicating ozone stabilization, there are no signs of a significant recovery of ozone layer thickness, so it can be expected that UV-B dose levels will remain high in the future.

KEY WORDS: Thermal environment · UV radiation · Climate change · Heat index · Wind chill index · Vojvodina region · Serbia

— Resale or republication not permitted without written consent of the publisher —

1. INTRODUCTION

Global climate change will lead to shifts in climate (IPCC 2007a) and will have manifold impacts on ecosystems in the coming decades (e.g. IPCC 2007b). A change in climatic conditions and variability, for example, extreme weather events (heat waves and droughts), is likely to occur more frequently in different spatial and time scales in the future (e.g. Mearns et al. 1997, Meehl & Tebaldi 2004, Rowell & Jones 2006, Beniston et al. 2007, Vidale et al. 2007, Laprise 2008). Therefore, assessments of climate change impacts on agro-ecosystem resources and functions

(water, climatic stresses, soil and landscape functions), the occurrence of new pests and plant diseases, and public health and potential adaptation measures at different spatial and time scales are important issues in climate change research (e.g. McMichael et al. 2003, Diffenbaugh et al. 2008, Eitzinger et al. 2009, Nemet 2010, Zhang & Cai 2011).

It is expected that climate change, among other factors, will have the following effects on human activities and quality of life: (1) extreme hot and cold conditions as the most significant factors in terms of human mortality and morbidity (Michelozzi et al. 2007, WHO 2008, Anderson & Bell 2009, Guo et al.

*Email: slavicans@neobee.net

2012); (2) pronounced changes in the thermal complex, comprising meteorological elements that will have a thermo-physiological effect on humans (Matzarakis & Mayer 2000, Laschewski & Jendritzky 2002, Matzarakis 2007, Jendritzky & Tinz 2009); and (3) increases in harmful solar UV radiation (280 to 320 nm, i.e. the UV-B region; Armstrong & Kricker 2001, Neale et al. 2003, De Fabo et al. 2004, Diffey 2004, Lucas et al. 2006). Solar UV radiation, especially in the UV-B range, which is strongly influenced by the ozone content in the atmosphere, has a large impact on life and materials on Earth (UNEP 2003). Although stratospheric ozone ceased its decline in 1996, primarily due to a reduction in chlorofluorocarbon (CFC) production (WMO 2011), elevated levels of harmful UV radiation are still regarded as a cause for concern. Because of the increasing concerns for humans and living organisms, it is necessary to (1) monitor and forecast UV-B radiation and (2) obtain data on UV radiation in the past to enable estimation of the long-term biological effects of this radiation (Reuder & Koepke 2005, Malinovic-Milicevic & Mihailovic 2011). To assess the severity of climate change effects on humans in terms of the effect of single climatic parameters, it is necessary to explore biometeorological indices, such as quantifiers of climate change effects. According to the WMO (2004), the relationship between climatic conditions, human activities and quality of life can be analyzed through the effect of UV-B radiation and the complex conditions of heat exchange, i.e. the thermal environment and air pollution. Because air pollution influences the UV-B dose and the thermal environment, all 3 factors have a synergistic impact on the aforementioned issues.¹ The term 'thermal environment' encompasses both atmospheric heat exchanges with the body and the body's physiological response. The term 'thermal environment' will henceforth include the effect of humidity and wind speed.

In this study we attempt to estimate the thermal environment and UV-B radiation indices in the Vojvodina region (northern Serbia). There are several studies that elaborate climate change issues for this region through (1) dynamic and statistical down-

scaling (Djurdjevic & Rajkovic 2008, Lalic et al. 2012, Rajkovic et al. 2012) and (2) examining the effect of climate change on crop yield (Lalic et al. 2012), the mosquito population (Petric et al. 2012), predominant enterovirus serotypes (Hrnjakovic et al. 2012), pests and plant diseases (Jevtic et al. 2012) and forests (Orlovic et al. 2012). Here we address the thermal environment and UV-B radiation indices, focusing on the spectrum of climate change issues that are highly important for this region. Pollution effects are not addressed in this study

Some key results presented here are based on surveys and case studies on climate change and on its influence on the environment, performed during the projects FP6 'ADAGIO' (2007–2009) (Eitzinger et al. 2009) and 'Studying climate change and its influence on the environment: impacts, adaptation and mitigation' (2011 to 2014) (Mihailovic 2012).

2. MATERIALS AND METHODS

2.1. Location and actual climate

The Vojvodina region is situated in the northern part of Serbia and the southern part of the Pannonian lowland (44° 37'–46° 11' N, 18° 51'–21° 33' E, and 75–641 m above sea level [a.s.l.], with the Fruska Gora mountains in the south). The region is the most important food production area in Serbia, with a total surface area of 21 500 km² (Fig. 1) and a population of ~2 million. The region has a continental climate, with some elements of a sub-humid and thermal climate (Katic et al. 1979). The mountains partially surrounding the Pannonian lowland have a significant effect on the basic climate characteristics of this lowland. However, exposure to air masses coming from the north and west, together with a huge range of temperatures throughout the year, means that the continental characteristics of Vojvodina's climate are more pronounced, particularly in the summer and winter (Lalic et al. 2011). The mean annual temperature is 11°C, and the mean annual precipitation is 602 mm (Mihailovic et al. 2004). According to Mihailovic et al. (2008), the Koppen climate formula for this region is *Cfbwx''*, where *C* = mild temperate/mesothermal climate; *f* = significant precipitation during all seasons; *w* = dry winters, i.e. the driest winter month's average precipitation is <1/10 the wettest summer month's average; *b* = warmest month's average is <22°C (but there are at least 4 mo averaging >10°C); and *x''* indicates that the second precipitation maximum occurs in autumn (Kottek et al. 2006).

¹From the monitoring reports for 7 cities in the Vojvodina region (2001–2008), it can be observed that traditional household heating, traffic and — partly — industry significantly influence air pollution through SO₂, NO₂ and black smoke (BS) pollutants. According to Malinovic-Milicevic (2012), the mean annual concentrations of these pollutants do not yet exceed critical levels, although elevated levels can nevertheless occur during the day

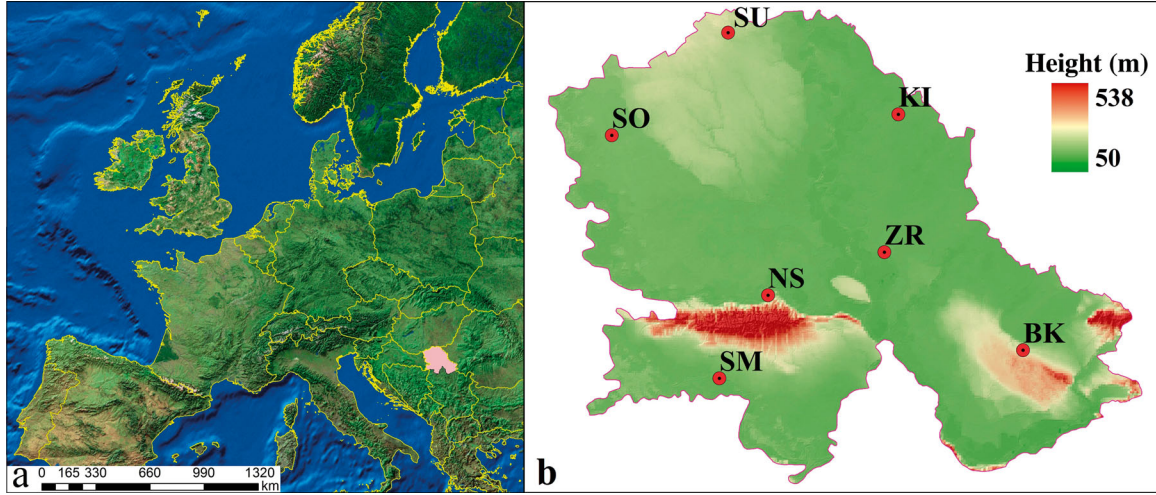


Fig. 1. (a) Vojvodina region (Serbia) in Europe and (b) the 7 sites used in the study: SO: Sombor, SU: Subotica; NS: Novi Sad; KI: Kikinda; ZR: Zrenjanin; BK: Banatski Karlovac and SM: Sremska Mitrovica

2.2. Data sources

To describe the actual climate conditions in the Vojvodina region, we used data from the weather station network of the Republic Hydrometeorological Institute of Serbia for Novi Sad, Subotica, Sombor, Kikinda, Zrenjanin, Banatski Karlovac and Sremska Mitrovica for the reference period 1992–2008 (referred to as RP92-08). All of these stations are predominantly located in rural areas and provide continuous daily data, including maximum and minimum temperatures, sunshine hours, precipitation, mean daily water vapor pressure and wind speed. We calculated the (1) mean annual temperature, (2) mean annual precipitation, (3) mean temperature for the hot (April to September) period and (4) for the cold period (October to March), (5) mean precipitation for the hot and (6) cold period, and (7) frequency of hot ($T_{\max} > 30^{\circ}\text{C}$) and (8) cold days ($T_{\max} < 0^{\circ}\text{C}$).

Data on expected climate conditions were obtained by applying a statistical downscaling technique on outputs used from the global climate model (GCM). The GCM used in this paper was developed at the Max-Planck Institute for Meteorology (ECHAM5) (Roeckner et al. 2003). The first step in an assessment of climate change effects on humans and their activities, and on living organisms is the downscaling of climate model outputs. For this purpose, either statistical or dynamical downscaling techniques are used. To synthesize the daily weather data series, the Met&Roll weather generator (Dubrovsky 1996, 1997) was used to statistically downscale the ECHAM5 model outputs using the A2 scenario for greenhouse

gas emissions for the year 2040 (referred to as PY2040). The change in global mean temperature is estimated using the middle (2.6°C) climate sensitivity. To calibrate and validate the Met&Roll weather generator, we analyzed 4 variable weather data series (daily sum of global radiation, maximum and minimum daily temperature, wind speed and water vapor pressure daily average) for the main climatic stations in the Vojvodina region. More details about these procedures can be found in Lalic et al. (2012).

The thermal complex was analyzed using indices recommended by the WMO (2004), i.e. the wind chill index (WCI) and the heat index (HI). The WCI is commonly used as a winter-time index to measure the heat that the atmosphere is capable of absorbing from an exposed surface. It was calculated according to Osczevski & Bluestein (2005):

$$\text{WCI} = 35.74 + 0.6215T_c - 35.75v^{0.16} + 0.4275T_cv^{0.16} \quad (1)$$

where T_c is air temperature ($^{\circ}\text{C}$) and v is wind velocity (m s^{-1}). The HI is a measure of how hot it feels when a certain ambient temperature and humidity are combined. It was calculated using the US National Climatic Data Centre (NCDC) formula and table generated by Steadman (1979, 1984):

$$\begin{aligned} \text{HI} = & -42.379 + 2.04901523T_F + 10.14333127\text{RH} \\ & - 0.22475541T_F\text{RH} - 6.83783 \times 10^{-3}T_F^2 \\ & - 5.481717 \times 10^{-2}\text{RH}^2 + 1.22874 \times 10^{-3}T_F^2\text{RH} \\ & + 8.5282 \times 10^{-4}T_F\text{RH}^2 - 1.99 \times 10^{-6}T_F^2\text{RH}^2 \end{aligned} \quad (2)$$

where T_F is air temperature in $^{\circ}\text{F}$ and RH is relative humidity in %. This formula is effective when the air

temperature is $>26.7^{\circ}\text{C}$ ($>80^{\circ}\text{F}$) and the relative humidity is $\geq 40\%$. The WCI and HI are always calculated using temperature, relative humidity and wind speed at 7, 14 and 21 h (local time) for selected places.

Due to the lack of measurement sites for UV-B radiation and the UV index (UVI) in the Vojvodina region, for the purpose of this paper we have included (1) values measured in Novi Sad (45.33°N , 19.85°E , 84 m a.s.l.) using the broadband Yankee UVB-1 biometer, (2) values calculated using the parametric numerical model NEOPLANTA (Malinovic et al. 2006, Malinovic-Milicevic & Mihailovic 2011) and (3) values calculated using an empirical formula based on a linear correlation between the daily sum (dose) of the UV-B (UVB_d) and the daily sum of the global solar radiation (G_d) in kJ m^{-2} (Feister & Grasnack 1992, Koronakis et al. 2002, Basset & Korany 2007, Malinovic-Milicevic 2012). More details about the model, NEOPLANTA, are provided in Appendix 1. The empirical formula, which is derived on the basis of the relationship between the daily values of UVB_d (measured UVI data and the corresponding calibration factors) and G_d (calculated via an empirical formula) for the period April 2003 to December 2009 in Novi Sad (correlation coefficient $R = 0.964$), has the form:

$$\text{UVB}_d = 0.002507G_d - 5.985 \quad (3)$$

Using this formula, we calculated the UVB_d values for the selected places for the period 1981–2008.

Finally, we briefly discuss the accuracy of the methods used in this paper. Taking into account the error for the calibration constant and the error of quantization and conversion to erythemal weighted UV-B irradiance, the estimated maximal error of the UV-B measurements is $<9\%$ (Malinovic et al. 2006). The accuracy of the NEOPLANTA model was tested by comparing the calculated and measured UVI. A simple inspection of the data indicates that the absolute difference between the model outputs and measurements (cloudiness ≤ 0.2) was in the interval ± 0.5 UVI for 95% of the data (Malinovic et al. 2006). Under all amounts of cloudiness, a strong Pearson correlation of 0.85 was found between the measured data and the NEOPLANTA outputs (Malinovic-Milicevic & Mihailovic 2011). Finally, verification of empirical Eq. (3) was performed by comparing the standard deviations and the Pearson coefficient of correlation between the calculated and measured values. A very strong Pearson correlation (0.96) and a small difference between standard deviations (3.7%) indicate the reliability of this formula (Malinovic-Milicevic 2012).

3. RESULTS AND DISCUSSION

3.1. Comparison of the actual climate with the climate projection (A2 scenario)

Over the last 50 yr, atmospheric warming has accelerated in the Vojvodina region. During the 1981–2008 period, records indicate a strong temperature gradient in the SE–NW direction as well as positive and negative precipitation trends. One possible explanation for the occurrence of these trends is the increased number of extreme weather events during this period. For example, in Novi Sad in 1999, due to a few extreme precipitation events, the annual precipitation was 50% above the long-term average, whereas in 2000, the annual precipitation was 50% below the long-term average due to an extremely dry spring and summer. Thus the most pronounced characteristic of the climate in the Vojvodina region during the RP92-08 period was an increased variability, particularly for precipitation (Lalic et al. 2012). The mean annual temperature during the RP92-08 period was 11.6°C , whereas the mean annual precipitation was 605.2 mm. The comparison of the PY2040 model outputs against the observations for the RP92-08 period (Fig. 2) indicate that a warmer and drier climate in the Vojvodina region can be expected in the future. More specifically, Fig. 2 indicates the following (1) there will be an increasing trend in mean annual temperature (Novi Sad: 8.6% to Sombor: 12.3%) (Fig. 2a), (2) the mean annual precipitation will have a decreasing trend (in the range of Zrenjanin: 8.1% to Novi Sad and Banatski Karlovac: 14.2%) (Fig. 2b), (3) the frequency of hot days will be higher (from Novi Sad: 29.4% to Sombor: 50%) (Fig. 2c) and (4) the frequency of cold days will decrease (in the range of Sombor: 11.8% to Banatski Karlovac: 27.8%) (Fig. 2d). Calculations from the model outputs also indicate (1) a higher increase, on average, of the mean temperature for the cold period (24.9%) compared to the mean temperature of the hot period (6.7%) and (2) a reduction in precipitation during the growing season (15.7%).

3.2. Thermal complex

The monthly distribution for the absolute daily maximum heat index (HI_{ad}) and minimum wind chill index (WCI_{ad}) (Li & Chan 2000) over the RP92-08 period is depicted in Fig. 3. A significant negative minimum occurs between October and March, and a large positive maximum occurs between April and

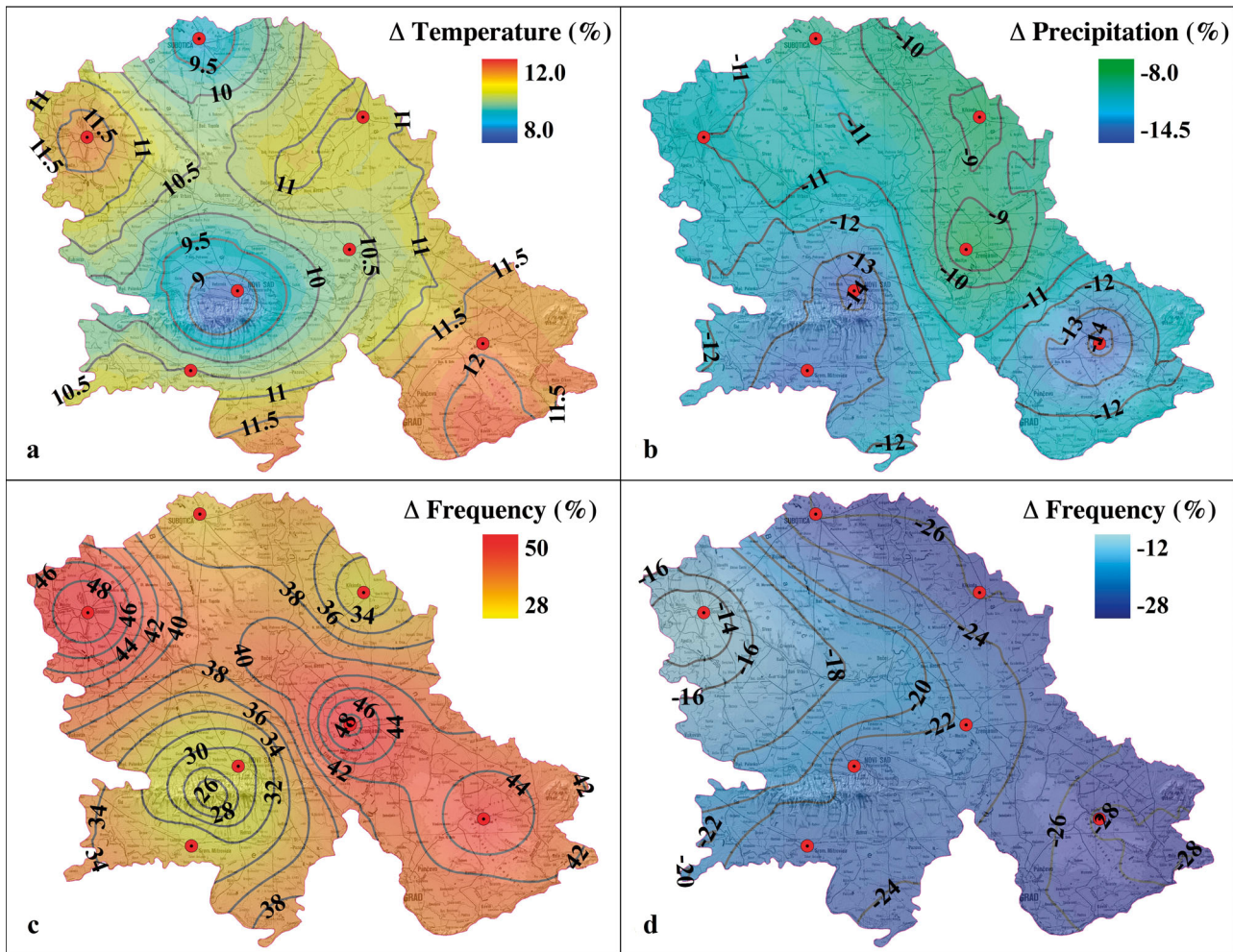


Fig. 2. Relative changes (%) in (a) mean annual temperature, (b) mean annual precipitation, (c) frequency of hot and (d) cold days in the Vojvodina region (PY2040 model outputs compared to the observed values for the RP92-08 period). Study sites (red dots) as in Fig. 1

October ($HI_{ad} > 27^{\circ}\text{C}$). The absolute minimum WCI_{ad} (-29.8°C) was recorded in Subotica on 13 January 2003. The temperature, relative humidity and wind speed recorded at the time of the absolute minimum WCI_{ad} were -22.8°C , 81% and 2.4 m s^{-1} , respectively. The absolute maximum HI_{ad} (43.8°C) was recorded in Zrenjanin on 24 July 2007, with air temperature, relative humidity and wind speed of 42.1°C , 23% and 4.4 m s^{-1} , respectively.

The thermal conditions described by the WCI and HI are more pronounced during the winter (December to February) and summer (June to August) months. Therefore, the mean WCI and HI values for these periods are the best indicators of average thermal conditions. Their spatial distributions are presented in Fig. 4. From this figure, it is observable that Kikinda and Subotica are places with unfavorable

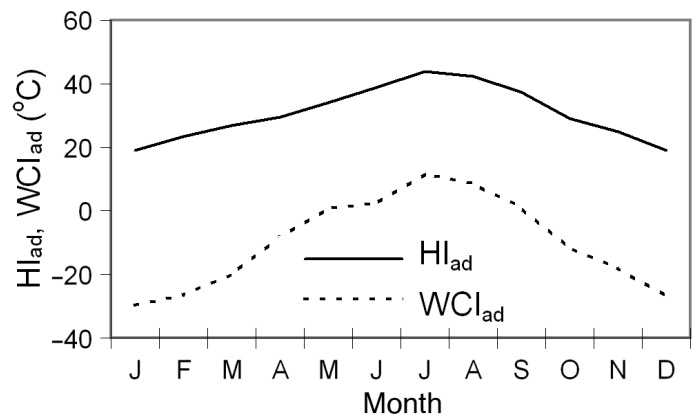


Fig. 3. Monthly distribution of absolute daily maximum heat index (HI_{ad}) and minimum wind chill index (WCI_{ad}) in the Vojvodina region for the RP92-08 period

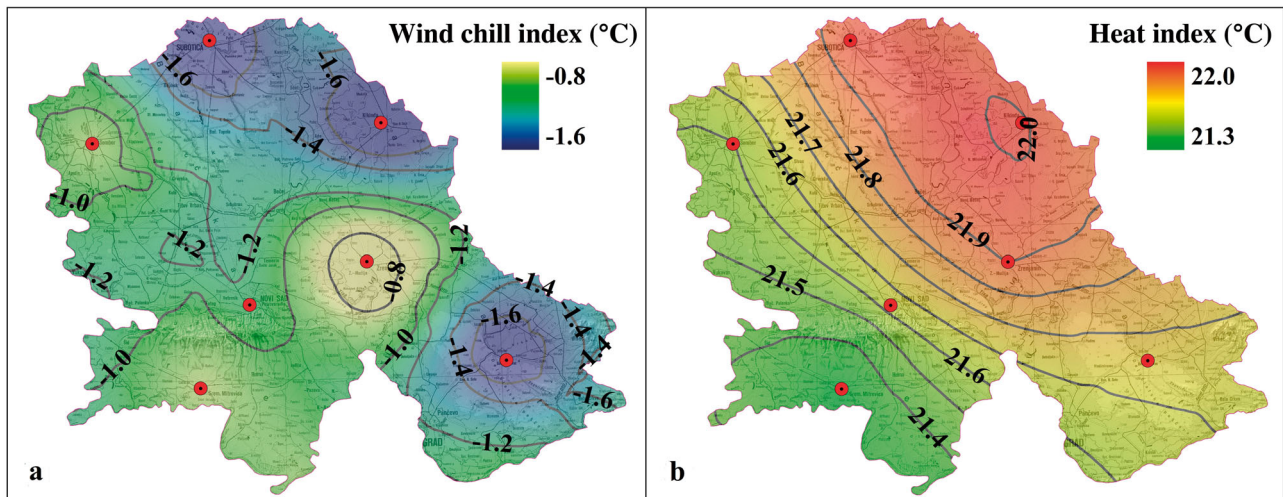


Fig. 4. Spatial distributions of the (a) wind chill index (WCI) for the winter months (Dec–Feb) and (b) heat index (HI) for the summer months (Jun–Aug) in the Vojvodina region for the RP92-08 period. Study sites (red dots) as in Fig. 1

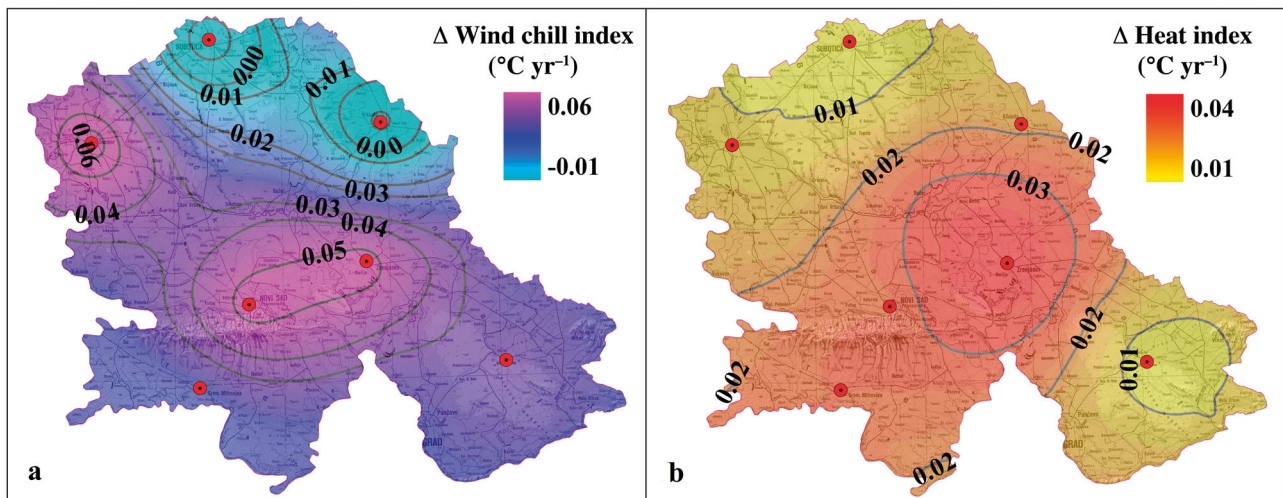


Fig. 5. Trends for the (a) wind chill index (WCI) for the winter months (Dec–Feb) and (b) heat index (HI) for the summer months (Jun–Aug) in the Vojvodina region for the RP92-08 period. Study sites (red dots) as in Fig. 1

thermal conditions, with the lowest WCI and highest HI values.

To analyze the long-term trends of the WCI and HI during the winter and summer months in the Vojvodina region for the RP92-08 period, we used linear regression. The WCI trend (Fig. 5a) decreases going towards the north, with a value of $-0.01^{\circ}\text{C yr}^{-1}$ at Kikinda and Subotica. The belt extending from the central towards the northwestern region has the highest values ($0.06^{\circ}\text{C yr}^{-1}$ maximum). From Fig. 5b, it can be observed that the highest growth for the HI is around Zrenjanin ($0.04^{\circ}\text{C yr}^{-1}$). From this area, a

tendency of decreasing HI in all directions is evident. However, this trend is more enhanced in the northwest to southeast direction.

3.3. UV radiation

To investigate the long-term trend for UV-B radiation in the Vojvodina region, we calculated the annual averages for the estimated daily UV-B dose and total ozone for 1981 to 2008 using Eq. (3) and then averaged these values over all 7 sites. The

annual ozone amount was calculated using the daily values for Novi Sad, which were measured using a total ozone mapping spectrometer and the ozone monitoring instrument on NASA satellites (Nimbus-7, Meteor-3 and Earth Probe Aura) (NASA 2010). In further calculations, this value is used as a representative one for other places. The annual averages for the estimated daily UV-B dose and the total calculated ozone trends are depicted in Fig. 6a.

To determine the significance level (p) of each trend, we used the Mann–Kendall nonparametric test (Yue & Pilon 2004, Helsel & Frans 2006). This figure shows (1) a moderately decreasing trend in the total ozone since 1981 ($2.2\% \text{ decade}^{-1}$, $p = 0.002$) and (2) an increasing trend in the UV-B dose ($3.7\% \text{ decade}^{-1}$, $p = 0.019$). According to the WMO (2011), ozone ceased its decline in 1996. Therefore, in addition to the trend calculated for the 1981–2008 period, we have calculated the ozone trends for the periods 1981–1996 and 1997–2008. The ozone trend in the Vojvodina region for the 1981–1996 period declines by $4.2\% \text{ decade}^{-1}$ ($p = 0.013$). The trend for the period 1997–2008 nominally shows a stabilization of ozone but does not show recovery. However, we found that this trend is not statistically significant. According to the US Climate Change Science Program (CCSP 2008), an increase in the total ozone content between 60°N and 60°S is expected in response to the decrease in halogen loading, and is expected to be 2% above the 1980 values by 2100. According to the WMO (2011), measurements from some stations in unpolluted locations indicate that the UV radiation levels have been decreasing since the late 1990s. However, at some Northern Hemisphere stations, UV-B radiation is still increasing as a consequence of long-term changes to other factors that also affect UV-B radiation (WMO 2011).

In Fig. 6b, the annual variations in the daily averaged UV-B dose and monthly mean absolute daily maximum for the period 1981–2008 are depicted. The daily averaged UV-B dose is between 2.062 (December) and 58.773 kJ m^{-2} (June). The seasonal changes in the daily averaged UV-B dose are a result of differences in the daylight duration and solar zenith angle, whereas the daily changes are predominantly the result of changes in cloudiness and the ozone amount. The largest part of the annual dose of UV-B radiation in the Vojvodina region ($\sim 78\%$) occurs between April and September. The highest absolute maxima are recorded in June and July, and have remarkably larger values in May than in August. The UV-B dose extremes are a very useful parameter for planning human activities, for analyzing the quality of life and for different purposes in agriculture. Therefore, we focused our analyses on the hot period (April to September), which is when the UV-B doses reaching the ground in the Vojvodina region are the largest. We calculated the daily UV-B doses for the hot period during the period 1981–2008 using Eq. (3) and the corresponding linear trends per decade for all 7 sites to obtain maps for the Vojvodina region. From Fig. 7a, it can be observed that small differences exist in the daily UV-B dose values for the hot period between sites ($\sim 3\%$). A further inspection of this figure indicates that the highest values of daily UV-B doses for the hot period are in the eastern part of the region (Banatski Karlovac and Kikinda: 45.146 kJ m^{-2}), whereas the lowest are in the western part of the Vojvodina region (43.842 kJ m^{-2} for Sombor). Finally, Fig. 7b shows that the highest trends of daily UV-B doses for the hot period are in Novi Sad (5.6%) and Zrenjanin (5.1%), whereas the lowest trend is in Banatski Karlovac (3.3%).

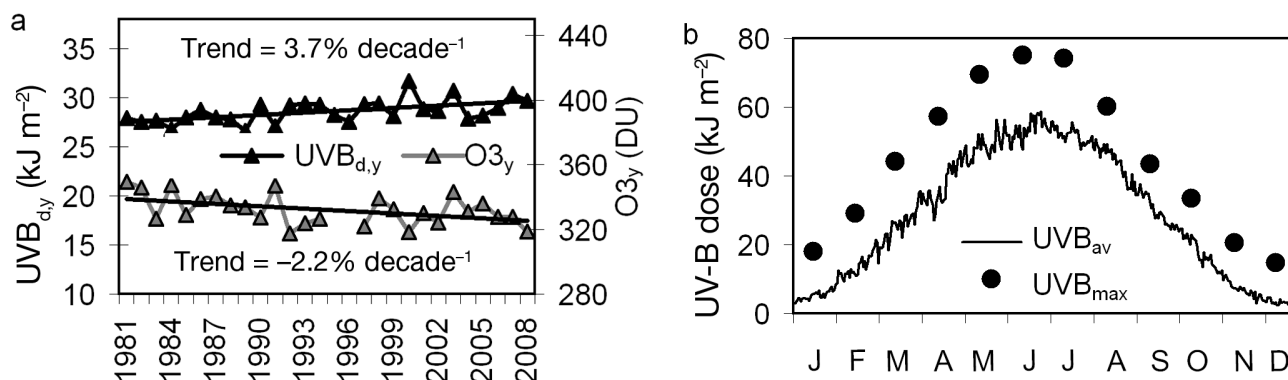


Fig. 6. (a) Annual averages of the estimated daily UV-B dose ($UVB_{d,y}$) and total ozone ($O3_y$, in Dobson units, DU) trends. (b) daily averaged UV-B dose and monthly mean absolute daily maximum UV-B dose (UVB_{av} and UVB_{max} , respectively) in the Vojvodina region for the period 1981–2008

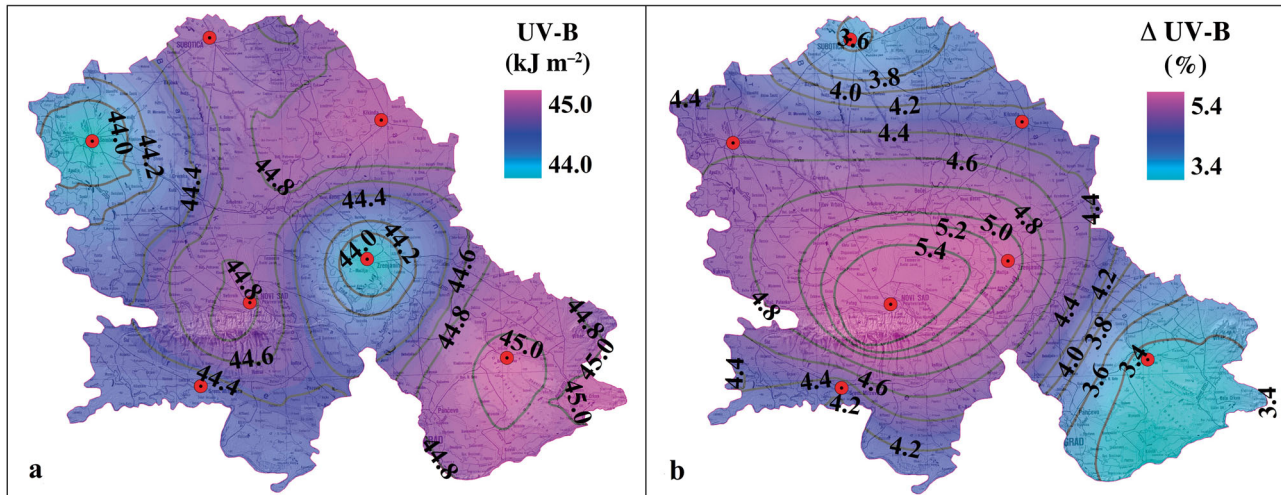


Fig. 7. Spatial distribution of (a) annual the estimated daily UV-B doses for the hot period (Apr–Sep) and (b) the trend per decade (%) of these doses in the Vojvodina region for the period 1981–2008. Study sites (red dots) as in Fig. 1

4. CONCLUSIONS

In this study, we considered the thermal environment and UV-B radiation indices in the Vojvodina region, Serbia to offer evidence for assessing the direct and indirect effects of climate change on human activities in this region. The following points can be made.

(1) We described actual climate conditions using data from the network of the Republic Hydrometeorological Institute of Serbia for 7 sites for the period 1992–2008 ($Cfwbx$ formula, according to Köppen classification).

(2) We applied a statistical downscaling technique on outputs used from the ECHAM5 under the A2 scenario to make a projection on the climate for the year 2040, which indicates that in the future, a warmer and drier climate in the Vojvodina region can be expected. From the evidence, which is expressed through ranges of spatial changes, it can be observed that (i) the mean annual temperature (8.6 to 12.3%) and frequency of hot days will increase (29.4 to 50%); (ii) the mean annual precipitation (8.1 to 14.2%) and frequency of cold days will decrease (11.8 to 27.8%); (iii) the mean temperature for the cold period (24.9%) will increase more significantly compared to the mean temperature for the hot one (6.7%); and (iv) a reduction in precipitation will occur in the growing season (15.7%).

(3) We analyzed the thermal complex during the period 1992–2008 using indices recommended by the WMO, i.e. the WCI and HI for the winter (December to February) and summer (June to August) periods.

At all sites, HI has a tendency to increase. The cities Kikinda and Subotica have the most unfavorable thermal conditions (the lowest WCI and highest HI) in the Vojvodina region.

(4) We analyzed the trend for the UV-B dose using (i) values measured in Novi Sad (Yankee UVB-1 biometer), (ii) values calculated using the parametric numerical model NEOPLANTA and (iii) values calculated using an empirical formula we derived on the basis of a linear correlation between the daily UV-B dose and the daily sum of the global solar radiation. We propose that this method will be useful for establishing time series of the UV-B doses in regions with a sparse distribution of places in the network for monitoring UV-B radiation. We determined an increase in UV-B of 3.7% decade⁻¹. However, even though there is some evidence indicating ozone stabilization, there are no signs of a significant recovery of ozone layer thickness. Therefore, it can be expected that UV-B dose levels will remain high in the future.

Acknowledgements. The research presented in this paper was performed as a part of the project 'Studying climate change and its influence on the environment: impacts, adaptation and mitigation' (No. III 43007), supported by the Ministry of Education and Science of the Republic of Serbia within the framework of integrated and interdisciplinary research over the period 2011–2014. The authors are grateful to the Provincial Secretariat for Science and Technological Development of Vojvodina for the support under the project 'Climate projections for the Vojvodina region up to 2030 using a regional climate model' (Project no. 114-451-2151/2011-01). Some of this research was conducted as a part of activities in the framework of the Transport and Urban Development COST Action TU0902.

LITERATURE CITED

- Anderson G, Bell M (2009) Weather-related mortality: how heat, cold, and heat waves affect mortality in the United States. *Epidemiology* 20:205–213
- Armstrong BK, Kricger A (2001) The epidemiology of UV induced skin cancer. *J Photochem Photobiol B* 63:8–18
- Basset HA, Korany MH (2007) The global and UV-B radiation over Egypt. *Atmosfera* 20:341–358
- Beniston M, Stephenson DB, Christensen OB, Ferro CAT and others (2007) Future extreme events in European climate: an exploration of regional climate model projections. *Clim Change* 81:71–95
- Bird ER, Riordan C (1986) Simple solar spectral model for direct and diffuse irradiance on horizontal and tilted planes at the earth's surface for cloudless atmosphere. *J Clim Appl Meteorol* 25:87–97
- Brine DT, Iqbal M (1983) Solar spectral diffuse irradiance under cloudless skies. *Sol Energy* 30:447–453
- CCSP (2008) Trends in emissions of ozone-depleting substances, ozone layer recovery, and implications for ultraviolet radiation exposure. In: Ravishankara AR, Kurylo MJ, Ennis CA (eds) A Report by the US Climate Change Science Program and the Subcommittee on Global Change Research. Department of Commerce, NOAA's National Climatic Data Center, Asheville, NC
- De Fabo EC, Noonan FP, Fears T, Merlino G (2004) Ultraviolet B but not ultraviolet A radiation initiates melanoma. *Cancer Res* 64:6372–6376
- Diffenbaugh NS, Giorgi F, Pal JS (2008) Climate change hotspots in the United States. *Geophys Res Lett* 35: L16709, doi:10.1029/2008GL035075
- Diffey B (2004) Climate change, ozone depletion and the impact on ultraviolet exposure of human skin. *Phys Med Biol* 49:R1
- Djordjevic V, Rajkovic B (2008) Verification of a coupled atmosphere–ocean model using satellite observations over the Adriatic Sea. *Ann Geophys* 26:1935–1954
- Dubrovsky M (1996) Met&Roll: the stochastic generator of daily weather series for the crop growth model. *Meteorologicke Zpravy* 49:97–105
- Dubrovsky M (1997) Creating daily weather series with use of the weather generator. *Environmetrics* 8:409–424
- Eitzinger J, Kubu G, Thaler S, Alexandrov V and others (2009) Final report, including recommendations on adaptation measures considering regional aspects. Final scientific report of the ADAGIO project: adaptation of agriculture in European regions and environmental risk under climate change. Specific Support Action, FP6-2005-SSP-5-A, Proj No 044210, 6th Framework Programme (European Commission). Institute of Meteorology, BOKU, Vienna
- Feister U, Grasnack KH (1992) Solar UV radiation measurements at Potsdam (52° 22' N, 31° 5' E). *Sol Energy* 49: 541–548
- Guo Y, Punnasir K, Tong S (2012) Effects of temperature on mortality in Chiang Mai city, Thailand: a time series study. *Environ Health* 11:36
- Helsel DR, Frans LM (2006) Regional Kendall test for trend. *Environ Sci Technol* 40:4066–4073
- Hess M, Koepke P, Schult I (1998) Optical properties of aerosols and clouds: the software package OPAC. *Bull Am Meteorol Soc* 79:831–844
- Hrnjakovic IB, Cvjetkovic JP, Radovanov J, Milosevic VS (2012) Predominant enterovirus serotypes in the Vojvodina region (Serbia). In: Mihailovic DT (ed) Essays on Fundamental and Applied Environmental Topics. Nova Science Publishers, New York, NY, p 225–252
- IPCC (Intergovernmental panel on Climate Change) (2007a) Contribution of Working Group I to the Fourth Assessment Report of the IPCC. In: Solomon S, Qin D, Manning M, Chen Z and others (eds) Climate Change 2007: the physical science basis. Cambridge University Press, Cambridge
- IPCC (Intergovernmental panel on Climate Change) (2007b) Contribution of Working Group II to the Fourth Assessment Report of the IPCC. In: Parry ML, Canziani OF, Palutikof JP, van der Linden PJ, Hanson CE (eds) Climate change 2007: impacts, adaptation and vulnerability. Cambridge University Press, Cambridge
- Jendritzky G, Tinz B (2009) The thermal environment of the human being on the global scale. *Glob Health Action* doi: 10.3402/gha.v2i0.2005
- Jevtic R, Masirevic S, Vajgand D (2012) The impact of climate change on diseases and pests of small grains and sunflower in the Vojvodina Region (Serbia). In: Mihailovic DT (ed) Essays on Fundamental and Applied Environmental Topics. Nova Science Publishers, New York, NY, p 277–306
- Justus CG, Paris MV (1985) A model for solar spectral irradiance at the bottom and top of a cloudless atmosphere. *J Clim Appl Meteorol* 24:193–205
- Katic P, Djukanovic D, Djakovic P (1979) Climate of SAP Vojvodina. Institute for Field and Vegetable Crops, Faculty of Agriculture, University of Novi Sad, Novi Sad (in Serbian)
- Koronakis PS, Sfantos GK, Paliatsos AG, Kaldellis JK, Farofalakis JE, Koronaki IP (2002) Interrelations of UV-global/global/diffuse solar irradiance components and UV-global attenuation on air pollution episode days in Athens, Greece. *Atmos Environ* 36:3173–3181
- Kottek M, Grieser J, Beck C, Rudolf B, Rubel F (2006) World Map of the Köppen–Geiger climate classification updated. *Meteorol Z* 15:259–263
- Lalic B, Mihailovic DT, Podrascanin Z (2011) Future state of climate in Vojvodina (Serbia) and expected effects on crop production. *Field Vegetable Crop Res* 48:403–418 (In Serbian)
- Lalic B, Eitzinger J, Mihailovic DT, Thaler S, Jancic M (2012) Climate change impacts on winter wheat yield change: which climatic parameters are crucial in Pannonian lowland? *J Agric Sci CJO* 2012, doi:10.1017/S0021859612000640
- Laprise R (2008) Regional climate modelling. *J Comput Phys* 227:3641–3666
- Laschewski G, Jendritzky G (2002) Effects of the thermal environment on human health: an investigation of 30 years of daily mortality data from SW Germany. *Clim Res* 21:91–103
- Leckner B (1978) The spectral distribution of solar radiation at the earth's surface-elements of a model. *Sol Energy* 20: 143–150
- Li PW, Chan ST (2000) Application of a weather stress index for alerting the public to stressful weather in Hong Kong. *Meteorol Appl* 7:369–375
- Lucas RM, McMichael A, Smith W, Armstrong B (2006) Solar ultraviolet radiation. Global burden of disease from solar ultraviolet radiation. In: Pruss-Ustun A, Zeeb H, Mathers C, Repacholi MH (eds) Environmental Burden of Disease Series 13. WHO, Geneva

- Malinovic S, Mihailovic DT, Kapor D, Mijatovic Z, Arsenic I (2006) NEOPLANTA: a short description of the first Serbian UV index model. *J Appl Meteorol Climatol* 45: 1171–1177
- Malinovic-Milicevic S (2012) Monitoring of the non-ionizing radiation, air pollution and heat indexes in Vojvodina region. PhD thesis, University of Novi Sad (In Serbian)
- Malinovic-Milicevic S, Mihailovic DT (2011) The use of NEOPLANTA model for evaluating the UV index in the Vojvodina region (Serbia). *Atmos Res* 101:621–630
- Matzarakis A (2007) Climate, thermal comfort and tourism. In: Amelung B, Blazejczyk K, Matzarakis A (eds) *Climate change and tourism: assessment and coping strategies*. Maastricht-Warsaw-Frieburg, p 139–154
- Matzarakis A, Mayer H (2000) Atmospheric conditions and human thermal comfort in urban areas. *Proc 11th Seminar Environ Prot: Environ Health, Thessaloniki*, p 155–166
- McKinley AF, Diffey BL (1987) A reference action spectrum for ultraviolet induced erythema in human skin. *CIE Research Note. Comm Int d'Éclairage* 6:17–22
- McMichael AJ, Campbell-Lendrum DH, Corvalan CF, Ebi KL, Githeko A, Scheraga JD, Woodward A (2003) *Climate change and human health: risks and responses*. WHO, Geneva
- Mearns LO, Rosenzweig C, Goldberg R (1997) Mean and variance change in climate scenarios: methods, agricultural applications, and measures of uncertainty. *Clim Change* 35:367–396
- Meehl GA, Tebaldi C (2004) More intense, more frequent, and longer lasting heat waves in the 21st Century. *Science* 305:994–997
- Michelozzi P, Kirchmayer U, Katsouyanni K, Biggeri A and others (2007) Assessment and prevention of acute health effects of weather conditions in Europe, the PHEWE project: background, objectives, design. *Environ Health* 6:12
- Mihailovic DT (2012) Preface. In: Mihailovic DT (ed) *Essays on fundamental and applied environmental topics*. Nova Science Publishers, New York, NY, p 9–15
- Mihailovic DT, Lalic B, Arsenic I, Malinovic S (2004) Climate conditions for seed production. In: Milosevic M, Malesevic M (eds) *Seed breeding*, Vol. 1. Institute for Field and Vegetable Crops, Novi Sad (in Serbian)
- Mihailovic DT, Lalic B, Arsenic I (2008) Meteorological observations. Faculty of Agriculture, Institute for Field and Vegetable Crops, Novi Sad (in Serbian)
- NASA (2010) Total ozone mapping spectroradiometer, available at <http://ozoneaq.gsfc.nasa.gov/> (accessed 15 Dec 2010)
- Neale RE, Purdie JL, Hirst LW, Green AC (2003) Sun exposure as a risk factor for nuclear cataract. *Epidemiology* 14:707–712
- Nemet GF (2010) Cost containment in climate policy and incentives for technology development. *Clim Change* 103:423–443
- Orlovic S, Galic Z, Stojnic S, Klasnja B (2012) Monitoring of forest ecosystems in Serbia. In: Mihailovic DT (ed) *Essays on Fundamental and Applied Environmental Topics*. Nova Science Publishers, New York, NY, p 253–276
- Osczevski RJ, Bluestein M (2005) The new wind chill equivalent temperature chart. *Bull Am Meteorol Soc* 86: 1453–1458
- Petric D, Zgomba M, Bellini R, Becker N (2012) Surveillance of mosquito populations: a key element to understanding the spread of invasive vector species and vector-borne diseases in Europe. In: Mihailovic DT (ed) *Essays on Fundamental and Applied Environmental Topics*. Nova Science Publishers, New York, NY, p 193–224
- Rajkovic B, Veljkovic K, Djurdjevic V (2012) Dynamical downscaling: monthly, seasonal and climate case studies. In: Mihailovic DT (ed) *Essays on Fundamental and Applied Environmental Topics*. Nova Science Publishers, New York, NY, p 135–158
- Reuder J, Koepke P (2005) Reconstruction of UV radiation over Southern Germany for the past decades. *Meteorol Z* 14:237–246
- Roeckner E, Bäuml G, Bonaventura L, Brokopf R and others (2003) The atmospheric general circulation model ECHAM5. I. Model description. Rep 349, Max Planck Institute for Meteorology, Hamburg
- Rowell DP, Jones R (2006) The causes and uncertainty of future summer drying over Europe. *Clim Dyn* 27: 281–299
- Ruggaber A, Dlug R, Nakajima T (1994) Modeling of radiation quantities and photolysis frequencies in the troposphere. *J Atmos Chem* 18:171–210
- Steadman RG (1979) The assessment of sultriness. I. A temperature–humidity index based on human physiology and clothing science. *J Appl Meteorol* 18:861–873
- Steadman RG (1984) A universal scale of apparent temperature. *J Clim Appl Meteorol* 23:1674–1687
- UNEP (United Nations Environment Programme) (2003) *Environmental effects of ozone depletion and its interactions with climate change: 2002 assessment*. Vienna Convention for the Protection of the Ozone Layer and the Montreal Protocol on Substances that Deplete the Ozone Layer, Nairobi
- Vidale PL, Lüthi D, Wegmann R, Schär C (2007) European summer climate variability in a heterogeneous multimodel ensemble. *Clim Change* 81:209–232
- WHO (World Health Organization) (2008) *Improving public health responses to extreme weather / heat waves: EuroHEAT*. Meeting Rep, Bonn, 22–23 March 2007
- WMO (World Health Organization) (2004) *Guidelines on biometeorology and air quality forecasts*. WMO/TD No 1184 Geneva
- WMO (World Health Organization) (2011) *Scientific Assessment of Ozone Depletion: 2010*. Global Ozone Res Monit Proj–Rep No. 52, Geneva
- Yue S, Pilon P (2004) A comparison of the power of the *t*-test, Mann–Kendall and bootstrap tests for trend detection. *Hydrol Sci J* 49:21–37
- Zhang X, Cai X (2011) Climate change impacts on global agricultural land availability. *Environ Res Lett* 6:014014, doi:10.1088/1748-9326/6/1/014014

Appendix 1

The numerical model NEOPLANTA computes the direct and diffuse solar UV irradiances under cloud-free conditions for the wavelength range of 280 to 400 nm (with a 1 nm resolution) and the UV index. The effects of O₃, SO₂, NO₂, aerosols and 9 different ground surface types on UV radiation are included. The required input parameters are the local geographic coordinates and time or solar zenith angle, altitude and the amount of gases. Aerosols are incorporated into the model using the model OPAC, which provides the optical properties for 10 different aerosol types (Hess et al. 1998). Surface influence on UV irradiance was taken into account using spectral albedo values for 9 different surface types. The model includes its own vertical gas profiles and extinction cross-sections, extraterrestrial solar irradiance, aerosol optical properties and spectral surface reflectivity. The model uses standard atmosphere meteorological profiles but has the possibility of including real time meteorological data assimilated from high level resolution atmospheric mesoscale models. Output data are spectral direct, diffuse and global irradiance divided into the UV-A (320 to 400 nm) and UV-B (280 to 320 nm) regions of the spectrum. Biologically active UV irradiance is calculated using the erythral action spectrum of McKinley & Diffey (1987), UV index, spectral optical depth, and spectral transmittance for each atmospheric component.

The UV irradiance is calculated as the sum of the direct and diffuse components. The calculation of the direct region of radiation is performed using the Beer–Lambert law. The direct irradiance $I_{\text{dir}}(\lambda)$ at wavelength λ received at ground level by unit area is given by:

$$I_{\text{dir}}(\lambda) = I_0(\lambda) T(\lambda) \quad (\text{A1})$$

where $I_0(\lambda)$ is the extraterrestrial irradiance corrected for the actual Sun–Earth distance and $T(\lambda)$ is the total transmittance, which includes O₃, SO₂, NO₂, aerosol and air transmittances. Each of these individual transmittances are calculated using the optical depth $\tau(\lambda)$, which is the product of the extinction coefficient $\beta(\lambda)$ and the ray path through the atmosphere (s):

$$T(\lambda) = \exp[-(\lambda)] = \exp[-\beta(\lambda)s] \quad (\text{A2})$$

The extinction coefficient of UV radiation (β) is calculated by the product of the cross-sectional area (σ) and the layer particle concentration (N):

$$\beta(\lambda) = \sigma(\lambda)N \quad (\text{A3})$$

The starting point for calculating the diffuse region of radiation is the set of equations from Bird and Riordan's spectral model (1986), which represents equations from previous parametric models (Leckner 1978, Brine & Iqbal 1983, Justus & Paris 1985), improved after comparisons with a rigorous radiative transfer model and with measured spectra. The diffuse irradiance $I_{\text{dif}}(\lambda)$ is divided into 3 components: (1) the Rayleigh scattering component $I_{\text{ray}}(\lambda)$, (2) the aerosol scattering component $I_{\text{aer}}(\lambda)$ and (3) the component that accounts for the multi-

ple reflection of irradiance between the ground and the air $I_{\text{rf}}(\lambda)$:

$$I_{\text{dif}}(\lambda) = I_{\text{ray}}(\lambda) + I_{\text{aer}}(\lambda) + I_{\text{rf}}(\lambda) \quad (\text{A4})$$

The Rayleigh scattered component $I_{\text{ray}}(\lambda)$ of the diffuse region of UV irradiance is calculated as:

$$I_{\text{ray}}(\lambda) = I_0(\lambda)T_{\text{O}_3}(\lambda)T_{\text{SO}_2}(\lambda)T_{\text{NO}_2}(\lambda)T_{\text{aa}}(\lambda)[1 - T_{\text{ray}}^{0.95}(\lambda)]/2 \quad (\text{A5})$$

where T_{O_3} , T_{SO_2} , T_{NO_2} , T_{aa} and T_{ray} are the O₃, SO₂, NO₂, aerosol and air transmittances that have been defined by Eqs. (A2) and (A3). The transmittance of the aerosol absorption process, $T_{\text{aa}}(\lambda)$, is defined by (Justus & Paris 1985) as:

$$T_{\text{aa}}(\lambda) = \exp\{-[1 - \omega(\lambda)]\tau_a(\lambda)\} \quad (\text{A6})$$

where $\omega(\lambda)$ is the single-scattering albedo and $\tau_a(\lambda)$ is the aerosol optical thickness.

The aerosol-scattered irradiance is calculated as:

$$I_{\text{aer}}(\lambda) = I_0(\lambda)T_{\text{O}_3}(\lambda)T_{\text{SO}_2}(\lambda)T_{\text{NO}_2}(\lambda)T_{\text{aa}}(\lambda)T_{\text{ray}}^{1.5}(\lambda)[1 - T_{\text{as}}(\lambda)]D_s(\lambda) \quad (\text{A7})$$

where $T_{\text{as}}(\lambda)$ is the transmittance for aerosol scattering such that:

$$T_{\text{as}}(\lambda) = \exp[-\omega(\lambda)\tau_a(\lambda)] \quad (\text{A8})$$

and $D_s(\lambda)$ is the fraction of the scattered flux that is transmitted downwards. The function $D_s(\lambda)$ is dependent on the aerosol asymmetry factor (δ) according to Bird & Riordan (1986) and Justus & Paris (1985), as:

$$D_s = F_5 C_s \quad (\text{A9})$$

$$F_5 = 1 - 0.5 \exp[(B_1 + B_2 \cos\theta) \cos\theta] \quad (\text{A10})$$

$$B_1 = B_3[1.459 + B_3(0.1595 + B_3 \times 0.4129)] \quad (\text{A11})$$

$$B_2 = B_3[0.0783 + B_3(-0.3824 - B_3 \times 0.5874)] \quad (\text{A12})$$

$$B_3 = \ln(1 - \delta) \quad (\text{A13})$$

$$C_s(\lambda) = (\lambda + 0.55)^{1.8} \quad (\text{A14})$$

The asymmetry factor is a key optical characteristic of aerosols and is used from the OPAC database (Hess et al. 1998) for each wavelength and humidity.

The backscattered component of multiple reflections between the air and ground is calculated according to Bird & Riordan (1986):

$$I_{\text{rf}}(\lambda) = \frac{[I_{\text{dir}}(\lambda) + I_{\text{ray}}(\lambda) + I_{\text{aer}}(\lambda)]r_g(\lambda)r_s(\lambda)C_s(\lambda)}{1 - r_s(\lambda)r_g(\lambda)} \quad (\text{A15})$$

where $r_g(\lambda)$ is ground albedo and $r_s(\lambda)$ is sky reflectivity. Ground albedo is used from Ruggaber et al. (1994), whereas sky reflectivity is calculated by:

$$r_s(\lambda) = T'_{\text{O}_3}(\lambda)T'_{\text{aa}}(\lambda)\{0.5[1 - T'_{\text{ray}}(\lambda)] + [1 - F'_5(\lambda)]T'_{\text{ray}}(\lambda)[1 - T'_{\text{as}}(\lambda)]\} \quad (\text{A16})$$

where the primed transmittance terms are the regular atmospheric transmittance evaluated at an optical mass of 1.8.